Inorg. Chem. **2002**, *41*, 2202–2208

Discontinuum between a Thiolate and a Thiol Ligand

Danny G. McGuire, Masood A. Khan, and Michael T. Ashby*

Department of Chemistry and Biochemistry, The University of Oklahoma, 620 Parrington Oval, Room 208, Norman, Oklahoma 73019

Received October 22, 2001

The effect of H-bond donation to the thiolate ligand of (η^5-C_5H_5)Fe(CO)$_2$SR (**1**) to give H-bond adducts (**1·HX**) and eventually protonation to give [(η^5-C_5H_5)Fe(CO)$_2$(HSR)]$^+$ (**1H**$^+$) has been investigated experimentally and computationally. The electronic structures of **1(R = Me)**, several derivatives of **1(R = Me)·HX**, and **1(R = Me)H**$^+$ have been investigated using DFT (density functional theory) computational methods. As previously suggested, these calculations indicate the HOMO of **1** is Fedπ–Spπ antibonding and largely sulfur in character. The calculations indicate the electronic structure of **1** is not altered markedly by H-bond donation to the S center, but protonation results in a reorganization of the electronic structure of **1H**$^+$ and a HOMO that is largely metal in character. The reduction of Fe–S distances upon protonation of **1(R = Ph)** to give **1(R = Ph)H**$^+$**·BF$_4$**$^-$ (2.282(2) and 2.258(2) Å, respectively), as determined by single-crystal X-ray crystallography, also indicates diminished Fedπ–Spπ antibonding. Using the carbonyl stretching frequencies as a gauge of the donor ability of the thiolate ligand, we conclude that H-bonding has a continuous effect on the donor properties of the thiolate ligand of **1** (i.e., is a function of the pK_a of the H-bond donor). A discontinuous effect results when the pK_b of **1** is reached and the complex is protonated. For our study of **1**, the maximal effect of H-bonding is about 30% of protonation. Because the position of acid–base equilibrium depends on the relative basicities of the thiolate ligand and the conjugate base of the H-bond donor (and the relative heats of solvation of the acids and their conjugate bases), a true continuum of effects can be anticipated only for systems that are p*K*-matched in their given environments. Thus, when the conjugate base of the H-bond donor is a stronger base than the thiolate ligand (as in the present case), H-bond donation has a relatively small effect, but protonation triggers a large, discontinuous effect on the electronic structure of **1**.

Introduction

The observation of H-bonding to cysteinate ligands in metalloproteins[1] has fueled speculation that such dipole interaction may play a regulatory role. This has prompted the development of many small molecule models that incorporate intramolecular NH···S hydrogen bonds.[2−12] There is a consensus that dipole interactions decrease the donor properties of thiolate ligands,[13] and thiolate ligands that are protonated presumably experience a limiting effect.[14−18]

* To whom correspondence should be addressed. E-mail: mtashby@chemdept.chem.ou.edu.

(1) Hydrogen bonds to cysteinate ligands is indicated for copper proteins (e.g., plastocyanin: Guss, J. M.; Freeman, H. C. *J. Mol. Biol.* **1983**, *169*, 521), heme iron proteins (e.g., cytochrome P-450: Poulos, T. L.; Finzel, B. C.; Howard, A. J. *J. Mol. Biol.* **1987**, *195*, 687) and iron−sulfur proteins (e.g., rubredoxin: Day, M. W.; Hsu, B. T.; Joshuator, L.; Park, J. B.; Zhou, Z. H.; Adams, M. W. W.; Rees, D. C. *Protein Sci.* **1992**, *1*, 1494).
(2) Ueyama, N.; Taniuchi, K.; Okamura, T.; Nakamura, A.; Maeda, H.; Emura, S. *Inorg. Chem.* **1996**, *35*, 1945.
(3) Huang, J. O.; Ostrander, R. L.; Rheingold, A. L.; Walters, M. A. *Inorg. Chem.* **1995**, *34*, 1090.
(4) Walters, M. A.; Dewan, J. C.; Min, C.; Pinto, S. *Inorg. Chem.* **1991**, *30*, 2656.
(5) Chung, W. P.; Dewan, J. C.; Walters, M. A. *J. Am. Chem. Soc.* **1991**, *113*, 525.
(6) Ueno, T.; Kousumi, Y.; Yoshizawakumagaye, K.; Nakajima, K.; Ueyama, N.; Okamura, T.; Nakamura, A. *J. Am. Chem. Soc.* **1998**, *120*, 12264.
(7) Okamura, T.; Ueyama, N.; Nakamura, A.; Ainscough, E. W.; Brodie, A. M.; Waters, J. M. *J. Chem. Soc., Chem. Commun.* **1993**, 1658.
(8) Ueyama, N.; Nishikawa, N.; Yamada, Y.; Okamura, T.; Oka, S.; Sakurai, H.; Nakamura, A. *Inorg. Chem.* **1998**, *37*, 2415.
(9) Ueyama, N.; Yamada, Y.; Okamura, T.; Kimura, S.; Nakamura, A. *Inorg. Chem.* **1996**, *35*, 6473.
(10) Ueno, T.; Nishikawa, N.; Moriyama, S.; Adachi, S.; Lee, K.; Okamura, T.; Ueyama, N.; Nakamura, A. *Inorg. Chem.* **1999**, *38*, 1199.
(11) Kapteijn, G. M.; Grove, D. M.; Smeets, W. J. J.; Kooijman, H.; Spek, A. L.; Vankoten, G. *Inorg. Chem.* **1996**, *35*, 534.
(12) Ueno, T.; Ueyama, N.; Nakamura, A. *J. Chem. Soc., Dalton Trans.* **1996**, 3859.
(13) Caulton, K. G. *New J. Chem.* **1994**, *18*, 25.
(14) Sellmann, D.; Sutter, J. *ACS Symp. Ser.* **1996**, *653*, 101.
(15) Wander, S. A.; Reibenspies, J. H.; Kim, J. S.; Darensbourg, M. Y. *Inorg. Chem.* **1994**, *33*, 1421.
(16) Treichel, P. M.; Schmidt, M. S.; Crane, R. A. *Inorg. Chem.* **1991**, *30*, 379.

10.1021/ic011096g CCC: $22.00
Published on Web 03/26/2002

Given the weakened donor properties of thiolate ligands that bear H-bonds, the redox potentials of metals are influenced, and this is of profound significance with respect to redox-active metalloproteins. Most of our understanding of the effects of H-bonding to thiolates has been garnered from electrochemical measurements on the aforementioned model compounds.[3,18−21] Because such electrochemical experiments are carried out at high ionic strength, interpretation of the effects of H-bonding are complicated by the composite influence of the medium. This has prompted us to explore the donor properties of dipole-perturbed thiolate ligands using spectroscopic probes.[22] The carbonyl ligand is a sensitive reporter of electronic changes that take place at metal centers. Indeed, carbonyl ligands in metalloproteins and their model compounds have offered considerable insight into the electronic structures of their metal centers.[23] Other studies have employed carbonyl ligands to explore the effect H-bonding to chloride ligands has on their ability to π-stabilize unsaturated metal centers.[24] In the present study, we employ the electron-rich d^6 iron−thiolate complex **1** as a model for exploring the effects of Fe−S(R)···H−X interactions on the donor properties of the thiolate ligand in low-dielectric solvents. Hydrogen-bond donors (**HX**) yield adducts of **1** in solution (**1·HX**) that may be observed under equilibrium conditions. Sufficiently acidic compounds protonate **1** to give a thiol complex (**1H**$^+$). The effect of H-bond donation and eventual protonation of **1** (as reported by carbonyl stretching frequencies and modeled by density functional theory (DFT) calculation) is reported herein.

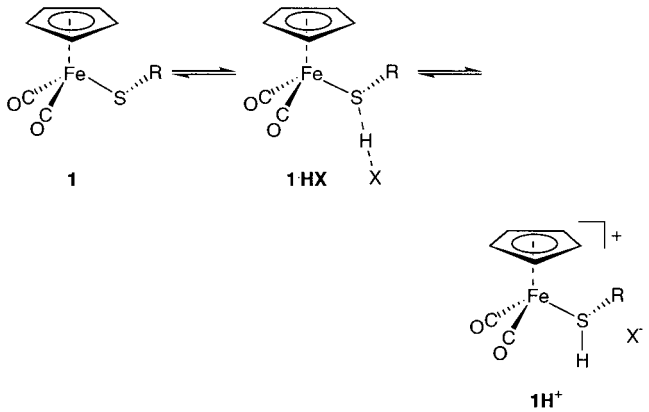

Experimental Section

Chemicals, Solvents, and General Procedures. All operations were carried out using Schlenk or glovebox techniques under argon or nitrogen unless stated otherwise. Hydrocarbon solvents were distilled from sodium/benzophenone, and CH_2Cl_2 was distilled from CaH_2. All solvents were degassed by three freeze−pump−thaw cycles before use. $CpFe(CO)_2SPh$, $CpFe(CO)_2Cl$, and $CpFe(CO)_2I$ were prepared by literature methods.[25−27] CH_3COOH, $CClH_2COOH$, CCl_2HCOOH, CCl_3COOH, CF_3COOH, and $HBF_4{\cdot}O(CH_3)_2$ were purchased from Aldrich Chemical Co. and used as received.

Instruments and References. ^{1}H NMR spectra were recorded on a Varian Inova 400 spectrometer. The NMR samples were prepared in tubes that had been glass-blown onto Schlenk adapters. The solutions were freeze−pump−thawed before flame-sealing under vacuum. ^{1}H NMR spectra were referenced to the residual solvent peak of $CDHCl_2$ (5.32 ppm). UV−vis spectra were recorded using a Hewlett-Packard HP8453 diode array spectrophotometer. Infrared spectra were recorded using a Bruker IFS 66/S FTIR with a DTGS detector.

Preparation of [CpFe(CO)$_2$(HSPh)]BF$_4$, 1(R = Ph)·HBF$_4$. A procedure different than that previously reported was employed to synthesize **1(R = Ph)·HBF$_4$**.[28] To a solution of **1(R = Ph)** (150 mg, 0.53 mmol) in CH_2Cl_2 (50 mL) was added $HBF_4{\cdot}O(CH_3)_2$ (64 μL, 0.53 mmol). The color of the solution changed immediately from red to yellow. After the solution was stirred for 5 min, pentane was added, and the product precipitated. The yellow powder was recovered using a Schlenk frit, and it was dried in vacuo for 4 h to give **1(R = Ph)·HBF$_4$** (170 mg, 0.46 mmol, 87% yield). The product was characterized by comparison of its NMR and IR spectra with those of an authentic sample. IR(CH_2Cl_2, cm^{-1}): ν_{CO} 2067, 2025. ^{1}H NMR (CH_2Cl_2, 400 MHz, 20 °C): δ 7.58−7.40 (m, Ph), 5.38 (s, SH), 5.34 (s, Cp).

UV−Vis and IR Measurements. Infrared spectroscopy measurements were made using a solution cell with NaCl plates and a 0.5 mm Teflon spacer. A quartz cell with a 0.2 mm path length was utilized in the UV−vis experiments. These path lengths permitted the same solutions to be employed for both measurements. All IR spectra were analyzed by taking the second derivative of each spectrum and then by fitting using the Gaussian amplitude method in the computer program Peakfit.[29] The spectra were in general fitted with the minimum number of Gaussian functions necessary to reproduce the line shapes. However, in a few cases, additional functions were employed when it was known by independent experiments that peaks overlapped to produce a symmetrical experimental peak. In such cases, the positions of the overlapping functions were fixed.

Intermolecular Interaction of 1 and 1H$^+$. Individual CH_2Cl_2 solutions of **1(R = Ph)** and **1(R = Ph)·HBF$_4$** (10 mM each) were prepared. The spectra that were obtained for these solutions were compared with the spectra of CH_2Cl_2 solutions of **1(R = Ph)** (10 mmol) to which less than 1 equiv of $HBF_4{\cdot}O(CH_3)_2$ was added. The spectrum of Figure S1, which resulted when 0.5 equiv of $HBF_4{\cdot}O(CH_3)_2$ was added, was satisfactorily fit with the parameters that

(17) Henderson, R. A.; Oglieve, K. E. *J. Chem. Soc., Dalton Trans.* **1998**, 1731.
(18) Allan, C. B.; Davidson, G.; Choudhury, S. B.; Gu, Z. J.; Bose, K.; Day, R. O.; Maroney, M. J. *Inorg. Chem.* **1998**, *37*, 4166.
(19) Sellmann, D.; Becker, T.; Knoch, F. *Chem. Eur. J.* **1996**, *2*, 1092.
(20) Farmer, P. J.; Reibenspies, J. H.; Lindahl, P. A.; Darensbourg, M. Y. *J. Am. Chem. Soc.* **1993**, *115*, 4665.
(21) Huang, J.; Ostrander, R. L.; Rheingold, A. L.; Leung, Y. C.; Walters, M. A. *J. Am. Chem. Soc.* **1994**, *116*, 6769.
(22) Rose, K.; Shadle, S. E.; Eidsness, M. K.; Kurtz, D. M.; Scott, R. A.; Hedman, B.; Hodgson, K. O.; Solomon, E. I. *J. Am. Chem. Soc.* **1998**, *120*, 10743.
(23) See, for example, infrared studied of hemoglobin (Dong, A. C.; Caughey, W. S. *Methods Enzymol.* **1994**, *232*, 139; Friedman, J. M. *Methods Enzymol.* **1994**, *232*, 205) and [NiFe]hydrogenases (Lai, C. H.; Lee, W. Z.; Miller, M. L.; Reibenspies, J. H.; Darensbourg, D. J.; Darensbourg, M. Y. *J. Am. Chem. Soc.* **1998**, *120*, 10103 and references therein).
(24) Yandulov, D. V.; Caulton, K. G.; Belkova, N. V.; Shubina, E. S.; Epstein, L. M.; Khoroshun, D. V.; Musaev, D. G.; Morokuma, K. *J. Am. Chem. Soc.* **1998**, *120*, 12553.
(25) Ahmad, M.; Bruce, R.; Knox, G. R. *J. Organomet. Chem.* **1966**, *6*, 1.
(26) Piper, T. S.; Cotton, F. A.; Wilkinson, G. *Inorg. Nucl. Chem.* **1955**, *1*, 165.
(27) Piper, T. S.; Cotton, F. A.; Wilkinson, G. *Inorg. Nucl. Chem.* **1956**, *3*, 104.
(28) Treichel, P. M.; Rosenhein, L. D. *Inorg. Chem.* **1981**, *20*, 942.
(29) *PeakFit*, Version 4.06; AISN Software Inc.: Saugus, MA, 1991.

Table 1. Crystal Structure Refinement Data for $CpFe(CO)_2SPh$ (**1(R = Ph)**) and $[CpFe(CO)_2(HSPh)](BF_4)$ (**1(R = Ph)·HBF$_4$**)

	1(R = Ph)	**1(R = Ph)·HBF$_4$**
chemical formula	$C_{13}H_{10}FeO_2S$	$C_{13}H_{11}BF_4FeO_2S$
fw	286.12	373.94
cryst syst	monoclinic	monoclinic
space group	$P2_1/n$	$P2_1/c$
a, Å	6.147(2)	6.3987(10)
b, Å	15.933(3)	7.4616(14)
c, Å	12.711(3)	31.177(5)
β, deg	97.92(3)	95.206(12)
V Å^3	1233.1(5)	1482.4(4)
Z	4	4
temp, K	188(2)	188(2)
λ, Å	0.71073	0.71073
ρ_{calcd}, g cm^{-3}	1.541	1.675
μ, mm^{-1}	1.376	1.202
R1, wR2 [$I > 2\sigma(I)$][a]	0.0536, 0.1437	0.0543, 0.1330
R1, wR2	0.0657, 0.1558	0.0785, 0.1637
GOF on F^2	1.122	1.092

[a] $R1 = \sum||F_o| - |F_c||/\sum|F_o|$; $wR2 = [\sum[w(F_o^2 - F_c^2)]/\sum[w(F_o^2)^2]]^{1/2}$; $w = 1/\sum[\sigma^2(F_o)^2+(aP)^2+(bP)^2+(cP)^2]$, $P = (F_o)^2[1/3 + [2(F_o)^2/3]]$ for $F_o^2 \geq 0$ (otherwise zero). $GOF = [\sum[w(F_o^2 - F_c^2)]/(n - m)]^{1/2}$, where n = no. of reflections observed and m = no. parameters.

were derived from individual spectra of the authentic samples of **1(R = Ph)** and **1(R = Ph)·HBF$_4$**.

Solutions of 1(R = Ph) with Incremental Concentrations of CCl_3COOH. Six CH_2Cl_2 solutions of **1(R = Ph)** (10 mM) with CCl_3COOH (0, 10, 50, 100, 500, 1000 mM) were prepared under nitrogen (Figure 3).

Solutions of 1(R = Ph) with the Same Concentration of Various Carboxylic Acids. Six CH_2Cl_2 solutions of **1(R = Ph)** (10 mM) with 150 mM CH_3COOH, $CClH_2COOH$, CCl_2HCOOH, CCl_3COOH, CF_3COOH, and $HBF_4{\cdot}O(CH_3)_2$ were prepared under nitrogen (Figure S2).

Solutions of $CpFe(CO)_2X$ (X = Cl,I) with CF_3COOH. Individual solutions of $CpFe(CO)_2X$ (X=Cl,I) (10 mM in CH_2Cl_2) were prepared. The spectra that were obtained for these solutions were compared with spectra of individual CH_2Cl_2 solutions of $CpFe(CO)_2X$ (X = Cl,I) (10 mmol) that also contained CF_3COOH (150 mM) (Table 4).

Solutions of 1(R = Ph) and $CpFe(CO)_2Cl$ in CH_2Cl_2 Solutions with Added Electrolyte. Individual CH_2Cl_2 solutions of $CpFe(CO)_2X$ (X = SPh,Cl) (10 mM each) were prepared. The spectra that were measured for these solutions were compared with the spectra of CH_2Cl_2 solutions of $CpFe(CO)_2X$ (X = Cl,I) (10 mmol) that also contained $(NBu_4)(PF_6)$ (1 M) (Table 4).

Solutions of 1(R = Ph) and CCl_3COOH with Added Electrolyte. Four CH_2Cl_2 solutions of **1(R = Ph)** (10 mM) with CCl_3COOH (0, 50, 100, 250 mM) were prepared under nitrogen. Sufficient $(NBu_4)(PF_6)$ was added to each of the solutions to give $[CCl_3COOH] + [(NBu_4)(PF_6)] = 1$ M (1.00, 0.95, 0.90, and 0.75 M, respectively). The IR spectra of the resulting solutions are illustrated in Figure S3.

X-ray Crystal Structures of 1(R = Ph) and 1(R = Ph)·HBF$_4$. Crystals of **1(R = Ph)** and **1(R = Ph)·HBF$_4$** suitable for analysis by X-ray diffraction were obtained by evaporation of a saturated pentane and CH_2Cl_2 solution, respectively, under nitrogen. The conditions that were employed to collect and process the X-ray data are summarized in Table 1. Data for both crystals were collected at −85 °C using a Siemens P4 diffractometer and Mo Kα (λ = 0.71075 Å) radiation.[30] The data were corrected for

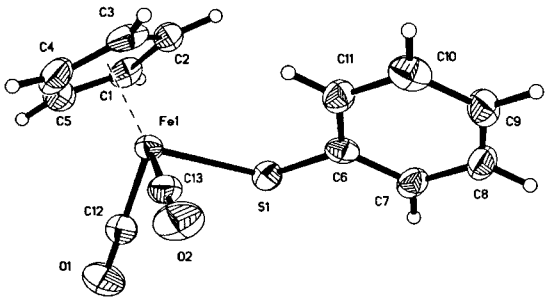

Figure 1. Thermal ellipsoid drawing of the crystal structure of **1(R = Ph)** at the 50% level with the labeling scheme.

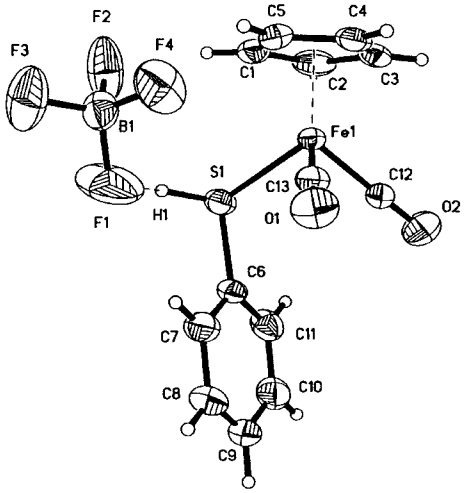

Figure 2. Thermal ellipsoid drawing of the crystal structure of **1(R = Ph)·HBF$_4$** at the 50% level with the labeling scheme.

Lorentzand polarization effects, and empirical absorption corrections based on ψ scans were applied.[31] Both structures were solved by direct methods and refined by least-squares on F^2 using all reflections using the SHELXTL (Siemens) system.[32] For **1(R = Ph)·HBF$_4$**, the hydrogen atom bound to S was located in a difference map, and it was refined isotopically. All other hydrogen atoms were included with idealized parameters. Thermal ellipsoid drawings of **1(R = Ph)** and **1(R = Ph)·HBF$_4$** are illustrated in Figures 1 and 2, respectively. The hydrogen atom H(1) on the S atom of **1(R = Ph)·HBF$_4$** forms a H-bond with F(1) of the BF_4^- anion as illustrated in Figure 2. Additional crystallographic results are summarized in Tables S1−S9.

Electronic Structure and Geometry Calculations. The molecular mechanics and molecular orbital calculations for **1(R = Me)**, **1(R = Ph)·HOOCF$_3$**, **1(R = Ph)·HBF$_4$**, and **1(R = Ph)H$^+$** were performed with SPARTAN 5.0 running on a Silicon Graphics IRIS Indigo 2 Solid Impact with an R10000 processor. The initial geometries were optimized using the Merck molecular force field (MMFF). The resulting geometries were refined using the semiempirical PM3(tm) method. Final geometries were obtained at the pBP/DF* level by optimization of all metric parameters. The perturbative Becke−Perdew method (pBP) is analogous to the BP method, but the gradient correction is introduced only after convergence based on the local potential alone has been achieved. DN* is a Gaussian basis set similar to 6-31G*, except five pure d-type functions are

(30) *Siemens XCSANS: X-ray Single-Crystal Analysis System*, Version 2.1; Siemens Analytical X-ray Instruments, Inc.: Madison, WI, 1994.

(31) North, A. C. T.; Phillips, D. C.; Mathews, F. S. *Acta Crystallogr.* **1968**, *A24*, 351.

(32) *SHELXTL Software Package for the Determination of Crystal Structures*, Release 5.1; Siemens Analytical X-ray Instruments, Inc.: Madison, WI, 1995.

used instead of six second-order Gaussians. The resulting coordinates of the computed structures of **1(R = Me)**, **1(R = Ph)·HOOCF$_3$**, **1(R = Ph)·HBF$_4$**, and **1(R = Ph)H$^+$** are available as Supporting Information (Tables S10−S13). Computed metric data for **1(R = Me)** and **1(R = Me)H$^+$** are compared with experimental data for **1(R = Ph)** and **1(R = Ph)·HBF$_4$** in Table 3. Computed vibrational frequencies are summarized in Table 4.

Results and Discussion

Model System. We will begin by explaining our choice of metal thiolate complex, solvent system, and H-bond donors that were employed in this study. We have previously shown that the organometallic complexes CpFe(CO)$_2$SR (**1**) are highly electron-rich, as evidenced by the high-lying first ionization potentials (IPs) observed in their gas-phase photoelectron spectra and the fact that they readily react with electrophiles such as alkyl halides[33] and electron-deficient alkynes.[34] The highest occupied molecular orbitals (HOMOs) of these complexes are Fe$d\pi$−Spπ antibonding and largely sulfur in character. Free-energy relationships have been observed between the HOMO IPs and the carbonyl stretching frequencies with respect to the rates of S_N2 electrophilic attack on sulfur.[33,34] Thus, the carbonyl stretching frequencies are direct reporters of the nucleophilicity of the sulfur. In the present study, we concern ourselves with the effects of dipolar H-bonding on the donor properties of the thiolate ligand. Because the addition of H-bond donors (Brønsted acids) to **1** can lead to decomposition of the complex, we employed relatively stable aryl derivative **1(R = Ph)** in this study. Alkyl derivatives of **1** tend to be less stable that aryl derivatives. It was desirable to employ nonpolar solvents in our measurements for two reasons. First, **1** is a relatively weak H-bond acceptor, and polar solvents tend to be competitive H-bond acceptors. Second, **1H$^+$** tends to undergo solvolysis with displacement of the relative weak thiol ligand. Thus, **1** has the added advantage (as an organometallic) of being soluble in nonpolar organic solvents. We initially employed CCl_4 as a solvent because it has been extensively used to study H-bonding effects,[35] but we found **1(R = Ph)** decomposes (via an apparent chain-radical mechanism) in CCl_4 to give the known dimer $[(CpFe(CO)_2)_2(S_2Ph_2)]^{2+}$.[36] We found no such problem with CH_2Cl_2. After investigating several classes of H-bond donors, we settled on carboxylic acids because they exhibited the appropriate range of H-bond donor ability and suitable solvent properties. We note from the outset that our discussion of the effects of adding carboxylic acids to CH_2Cl_2 solutions of **1** is restricted to analyzing trends. Whereas acid/base titrations in water can be treated quantitatively, the polar solutes that we employ have a significant effect on the properties of the solvents themselves. Furthermore, aggregation of polar solute molecules in nonpolar solvents can lead to localized effects. Accordingly, a quantitative analysis of the titration experiments that are described herein is not provided because of the inherent complexity of modeling dipolar reactions in a nonpolar environment.

Table 2. Selected Bond Distances (Å), Bond Angles (deg), and Torsional Angles (deg) for CpFe(CO)$_2$SPh **(1(R = Ph))** and [CpFe(CO)$_2$(HSPh)](BF$_4$) **(1(R = Ph)·HBF$_4$)**

	1(R = Ph)	1(R = Ph)·HBF$_4$
F1−S1	2.283(2)	2.259(1)
Fe1−C12	1.766(6)	1.819(3)
Fe1−C13	1.770(6)	1.789(3)
Fe1−Cp[a]	1.724(6)	1.711(3)
S1−C6	1.772(5)	1.776(4)
S1−H1		1.35(7)
S1−F1		3.363(4)
H1−F1		2.20(8)
Fe1−S1−C6	113.5(2)	111.2(2)
Fe1−C12−O1	178.3(6)	176.4(3)
Fe1−C13−O2	178.2(5)	178.4(3)
S1−Fe1−C12	87.1(2)	96.04(9)
S1−Fe1−C13	90.4(2)	94.19(9)
Cp−Fe1−S1	123.6(3)	120.4(1)
Cp−Fe1−C12	124.8(4)	122.1(1)
Cp−Fe1−C13	125.9(4)	123.5(1)
S1−H1−F1		147(3)
Cp−Fe1−S1−C6	86.4(3)	155.9(3)
C12−Fe1−S1−C6	−142.8(3)	−49.6(2)
C13−Fe1−S1−C6	−48.7(3)	44.1(2)
Fe1−S1−C6−C7	163.4(3)	93.6(4)
Fe1−S1−C6−C11	−17.8(5)	−89.4(3)

[a] Cp = centroid of the η^5-C_5H_5 ligand.

Effect of Protonation on the Molecular Structure of 1. To determine the effect of protonation on the molecular structure of **1** and to later calibrate the molecular orbital calculations, [CpFe(CO)$_2$(HSPh)](BF$_4$) (**1(R = Ph)·HBF$_4$**) was synthesized, and its molecular structure was determined by single-crystal X-ray crystallography. Apparently, the crystal structure of **1(R = Ph)·HBF$_4$** is the first of an Fe(II)−thiol complex to be reported, although there are several structures of Fe(III)−thiol complexes known, all porphyrin complexes.[37,38] For the sake of comparison, we also determined the structure of **1(R = Ph)**. The structure of **1(R = Et)** has been reported previously.[39] The structures of **1(R = Ph)** and **1(R = Ph)·HBF$_4$** are summarized in Tables 1 and 2. Thermal ellipsoid drawings of **1(R = Ph)** and **1(R = Ph)·HBF$_4$** are provided in Figures 1 and 2, respectively. Selected metric data for **1(R = Ph)** and **1(R = Ph)·HBF$_4$** are compared with relevant data from the literature in Table 3.

The crystal structure of Fe(TPP)(SPh)(HSPh) reveals that the Fe−S bond length for the Fe(III)−benzenethiolate group (2.27(2) Å) is shorter than that of the Fe(III)−benzenethiol group (2.43(2) Å).[38] This is not unexpected because a thiol is a weaker Lewis base than a thiolate. Remarkably, the Fe−S distance of **1(R = Ph)·HBF$_4$** is shorter than the corresponding distance for **1(R = Ph)**! We attribute the reduction of Fe−S distance from 2.282(2) Å for **1(R = Ph)**

(33) Ashby, M. T.; Enemark, J. H.; Lichtenberger, D. L. *Inorg. Chem.* **1988**, *27*, 191.
(34) Ashby, M. T.; Enemark, J. H. *Organometallics* **1987**, *6*, 1318.
(35) Raevsky, O. A. *J. Phys. Org. Chem.* **1997**, *10*, 405.
(36) Treichel, P. M.; Rosenhein, L. D. *Inorg. Chem.* **1984**, *23*, 4018.
(37) Byrn, M. P.; Katz, B. A.; Keder, N. L.; Levan, K. R.; Magurany, C. J.; Miller, K. M.; Pritt, J. W.; Strouse, C. E. *J. Am. Chem. Soc.* **1983**, *105*, 4916.
(38) Collman, J. P.; Sorrell, T. N.; Hodgson, K. O.; Kulshrestha, A. K.; Strouse, C. E. *J. Am. Chem. Soc.* **1977**, *99*, 5180.
(39) English, R. B.; Nassimbeni, L. R.; Haines, R. J. *J. Chem. Soc., Dalton Trans.* **1978**, 1379.

Table 3. Experimental and Computed Metric Data for $CpFe(CO)_2SR$ (**1**) and $[CpFe(CO)_2(HSR)]^+$ (**1H**$^+$)

cmpd	Fe−S	Fe−CO_{avg}	Fe−Cp	Fe−S−C	ref
Experimental					
$CpFe(CO)_2SEt$	2.296(2)	1.751(5)	1.76(1)	107.0(2)	39
$CpFe(CO)_2SPh$	2.283(2)	1.768(2)	1.724(6)	113.5(2)	*a*
$[CpFe(CO)_2(HSPh)](BF_4)$	2.259(1)	1.80(2)	1.711(3)	111.2(2)	*a*
Computed					
$CpFe(CO)_2SMe$	2.330	1.762(4)	1.757	106.1	*a*
$[CpFe(CO)_2(HSMe)]^+$	2.284	1.784(1)	1.752	112.5	*a*

[a] This study.

to 2.258(2) Å for **1(R = Ph)·HBF$_4$** to relief of the four-electron destabilization that results in Fedπ−Spπ antibonding in **1**. This interpretation is also supported by molecular orbital calculations that reproduce the observed trend in bond lengths (vide infra). We note a similar trend has been observed for (t-BuSH)$Cr(CO)_5$ versus its deprotonated analogue.[40] Other metric data of interest include the position of the H atom bound to the S atom of **1(R = Ph)·HBF$_4$**, which was located in a difference map and refined. The H atom is 1.35(7) Å from the S atom and 2.20(8) Å from a F atom of the BF_4^- counterion. The resulting S−H···F angle of 147(3)° suggests a nearly optimal dipolar interaction.[41]

Effect of Protonation on the Spectra of 1. Addition of 1 equiv of strong acids such as HBF_4·OMe_2 to solutions of **1(R = Ph)** in nonpolar solvents such as CH_2Cl_2 results in an immediate change in color from red to yellow, which corresponds to loss of the Fe−S LMCT band in the visible spectrum (cf. Figure 3, top). We have characterized the product of this reaction as the thiol complex $[CpFe(CO)_2(HSPh)](BF_4)$ (**1(R = Ph)·HBF$_4$**).[28] There is a corresponding increase in the carbonyl stretching frequencies upon protonation of **1**, which is consistent with a reduction in the donor ability of the thiol ligand with respect to the thiolate (Figure 3, middle). To interpret the experiments that will be described in the next section, it was important to establish whether the presence of **1H**$^+$ influences the spectra of **1**. The addition of less than 1 equiv of HBF_4·OMe_2 produces a mixture of **1** and **1H**$^+$ (Figure S1). The carbonyl stretching frequencies of **1(R = Ph)** are unperturbed under such conditions, which indicates no association of **1** and **1H**$^+$.

Effect of H-Bonding on the Spectra of 1. The addition of relatively weak acids of different effective acidities results in changes in the electronic and vibrational spectra that can be attributed to the equilibria of eq 1. Thus, an increase in the concentration of CCl_3COOH results in gradual loss of the Fe−S LMCT band in the electronic spectrum and a shift of the carbonyl vibrational modes to higher frequency. Rather than a discrete species, we intend **1·HX** to represent the continuum of change that takes place when the S−H−X H-bond is polarized from X to S. The absence of an isosbestic point at relatively low concentrations of carboxylic acid (before the appearance of **1H**$^+$) and the fact that the band-

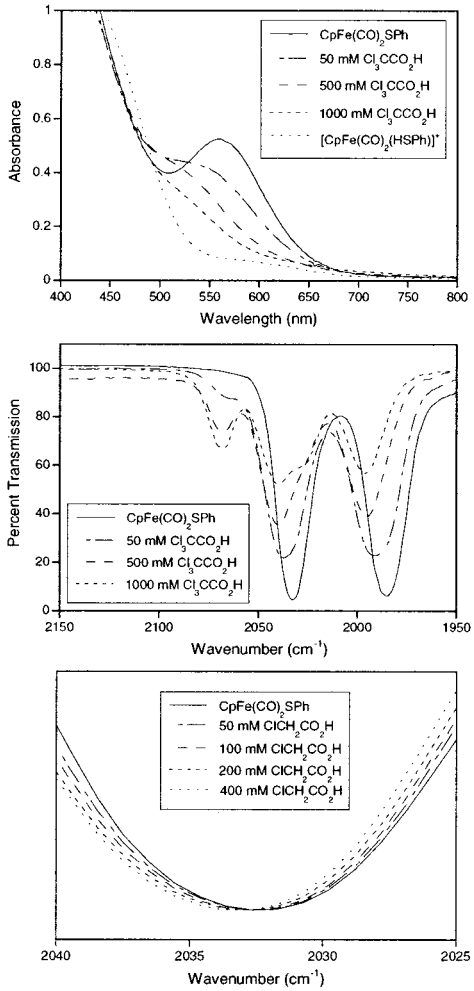

Figure 3. Top: changes in the UV−visible spectra of **1(R = Ph)** in CH_2Cl_2 upon addition of trichloroacetic acid. Note the lack of isosbestic points. The spectrum of **1(R = Ph)·HBF$_4$** is shown for comparison. Middle: corresponding changes in the IR spectra of the same solutions that were used to collect the UV−vis spectra. Bottom: normalized IR data that illustrate a shift in frequency without significant change in line width.

width of the asymmetric carbonyl vibrational mode remains constant while its maximum shifts to higher frequency (Figure 3, bottom) provide evidence for a continuum of change rather than a shift in equilibrium between discrete species **1** and **1·HX**. Such a polarization is expected to depend on several factors, including the relative polarities of the SH and XH bonds and the abilities of the medium to stabilize the species involved. Therefore, one might expect the equilibrium to shift to the right with the effective acidity of HX.[41,42] Indeed, for a given set of concentrations, we observe such a relationship experimentally (Table S2).

Maximum Effect of H-Bonding on the Donor Ability of a Thiolate Ligand. Although the range of acidities of the H-bond donors that were employed in this study in CH_2Cl_2 was immense, the acidities of H-bond donors in an aqueous environment are more restricted (by the autoprotolysis of water). We note that amide NH bonds, which are the conventional donors to cysteinate ligands in metalloproteins, are considerably less acidic than carboxylic acids.

(40) Darensbourg, M. Y.; Longridge, E. M.; Payne, V.; Reibenspies, J.; Riordan, C. G.; Springs, J. J.; Calabrese, J. C. *Inorg. Chem.* **1990**, *29*, 2721.

(41) Jeffrey, G. A. *An Introduction to Hydrogen Bonding*; Oxford University Press: New York, 1997.

(42) Jeffrey, G. A.; Saenger, W. *Hydrogen Bonding in Biological Structures*; Springer-Verlag: New York, 1991.

However, acidity is defined not only by the chemical nature of the species but also by its environment. The acidities (and basicities) of particular functional groups are known to vary several orders of magnitude within proteins, which is due in large part to the dielectric environment.[43] For example, the presence of a metal can lower the pK_a of the sulfhydryl group of cysteine by several pK units.[44] For the present case, evolution from a nonpolar to a polar dielectric environment is simulated by simply varying the concentration of a given H-bond donor (because the H-bond donors are more polar than the solvent itself). Thus, discrete species such as **1·HX** are not observed when [HX] is varied. Instead, a continuum of change is observed that reflects the combined influences of H-bond donation to the thiolate ligand and the polarity of the solvent environment (Figure 3). Eventually, the solvent environment becomes sufficiently polar to stabilize the conjugate acids and bases, and ionization occurs (i.e., protonation of the thiolate takes place). Equilibrium mixtures of **1·HX** and **1H**$^+$ (Figure 3, middle) reveal the upper limit of the effect of H-bonding on the donor properties of the thiolate ligand of **1**. Further differentiation of the relative basicities of S and X simply results in proton transfer to the S. The effects of H-bonding are continuous only to the "end point" of acid titration, at which point protonation occurs and a discrete change in the donor properties of the thiolate ligand takes place. Interestingly, the upper limit of the effect of H-bonding does not appear to be sensitive to the nature of X^-.

H-Bonding/Protonation versus Redox Potentials. It would be useful to understand the relative impact of H-bonding versus protonation on the redox potential of **1**. Unfortunately, **1**$^+$ rapidly dimerizes upon oxidation,[36] and irreversible cyclic voltammograms are obtained. Also, the thiol ligand of **1H**$^+$ is rapidly displaced by even weakly donating electrolytes. Furthermore, the aforementioned solvent dielectric effects complicate the interpretation. We have previously established a relationship between the first IP and F_{CO} of **1**:[33]

$$\mathrm{IP} = 2.68F_{CO} - 36.6 \quad (1)$$

Correlation between electrochemical and photoionization data generally yields empirical relationships of the form[45−49]

$$E_{1/2} = (0.6 \text{ to } 0.8)\mathrm{IP} - (3.5 \text{ to } 4.5) \quad (2)$$

Using the empirical formula

$$\Delta E_{1/2} = \lambda \Delta F_{CO} \text{ (i.e., for } 1.6 \le \lambda \le 2.1 \text{ and the observed } \Delta F_{CO} = 0.65 \text{ mdyn/Å}) \quad (3)$$

we predict a shift of the oxidation potential of **1** by 1.0−1.3 V upon protonation. This range may be compared with the 500−700 mV positive shift that has been observed for model Fe[19] and Ni[18] complexes upon protonation. While the absolute values of $\Delta E_{1/2}$ predicted by eq 3 may not be accurate, we are more concerned here with the relative importance of H-bonding versus protonation. It has been reported that the redox potentials of model Ni^{I}−thiolate complexes are shifted by +250 mV in polar solvents that are capable of H-bonding versus nonpolar solvents.[20] Unfortunately, the corresponding effects of protonation are not known for these systems. Furthermore, similar dielectric effects are observed for the redox potentials of molecules that are not expected to be significant H-bond acceptors. Using the value of $F_{CO} = 16.46$ mdyn/Å that is observed for **1·TFA**, we estimate a maximal effect of $300 \le \Delta E_{1/2} \le 400$ mV for H-bonding to **1**. This corresponds to an effect for H-bonding that is about 30% of that observed upon protonation.

Table 4. Experimental[a] (R = Ph) and Computed[b] (R = Me) Carbonyl Stretching Frequencies for (η^5-C_5H_5)Fe(CO)$_2$(SR), **1**, Its Hydrogen-Bonded Adducts, and Related Compounds

cmpd	acid	pK_a (in water)	obsd ν_{CO} (cm^{-1})		obsd F_{CO} (k_i) (mdyn/Å)	calcd ν_{CO} (cm^{-1})	
1H$^+$	HBF_4	<0	2069	2027	16.93_9 (0.34_7)	2068	2031[c]
1·TFA	F_3CCO_2H	<0.5	2040	1994	16.43_1 (0.37_4)	2035	1993
1·TCA	Cl_3CCO_2H	0.7	2039	1993	16.41_4 (0.37_4)		
1·DCA	Cl_2HCCO_2H	1.5	2035	1990	16.35_7 (0.36_5)		
1·CAA	ClH_2CCO_2H	2.9	2033	1986	16.30_9 (0.38_1)		
1·AcOH	H_3CCO_2H	4.8	2032	1985	16.29_2 (0.38_1)	2032	1990
1	none		2032	1985	16.29_2 (0.38_1)	2025	1980
FpCl[d]	none		2053	2007	16.64_3 (0.37_7)		
FpCl·TFA	F_3CCO_2H	<0.5	2058	2014	16.74_1 (0.36_1)		
FpCl	(NBu_4)(PF_6)		2053	2007	16.64_3 (0.37_7)		
FpI	none		2041	1996	16.45_5 (0.36_6)		
FpI	F_3CCO_2H	<0.5	2041	1996	16.45_5 (0.36_6)		

[a] Concentrations of 10 mM **1** and 175 mM acid in CH_2Cl_2. [b] Calculated at the pDF/BP* level for the Brønsted acid adducts of CpFe(CO)$_2$SMe using Spartan 5.0. The results of these calculations are available in the Supporting Information. [c] These are the vibrational frequencies for the naked **1H**$^+$ ion in the gas phase. The values of 2043 and 1998 were calculated for the tight ion pair **1·HBF$_4$**. [d] Fp = (η^5-C_5H_5)Fe(CO)$_2$.

It is noteworthy that the observed interaction between **1** and H-bond donors is not simply a dielectric effect in that (NBu_4)(PF_6) does not affect ν_{co}. Furthermore, the corresponding iodide complex is not influenced by acid (Table 4). There is an effect of acid on ν_{co} of the chloride derivative (consistent with the harder character of Cl^- vs I^-), albeit less significant than the effect on **1** under similar conditions. The series FpX may offer the opportunity to systematically investigate the effect of H-bond donation as a function of X. Although the addition of an "innocent" electrolyte such as (NBu_4)(PF_6) does not influence its spectra (Table 4), solvatochromism is observed for **1** (Table 5). There is an approximate linear dependence of λ_{max} on the dielectric constant of the solvent (Figure 5). This trend may be attributed to stabilization of the ground state (dipole stabilization of the antibonding HOMO of **1**, Figure 4) or Franck−Condon destabilization of the photoexcited state.[50] However,

(43) Fersht, A. *Enzyme Structure and Mechanism*; W. H. Freeman: New York, 1985.
(44) Hightower, K. E.; Huang, C. C.; Casey, P. J.; Fierke, C. A. *Biochemistry* **1998**, *37*, 15555.
(45) Lichtenberger, D. L.; Sellmann, D.; Fenske, R. F. *J. Organomet. Chem.* **1976**, *117*, 253.
(46) Gower, M.; Kane-Maguire, L. A.; Maier, J. P.; Sweigart, D. A. *J. Chem. Soc., Dalton Trans.* **1977**, 316.
(47) Byers, B. P.; Hall, M. B. *Organometallics* **1987**, *6*, 2319.
(48) Hubbard, J. L.; Lichtenberger, D. L. *J. Chem. Phys.* **1981**, *75*, 2560.
(49) Lichtenberger, D. L.; Elkadi, Y.; Gruhn, N. E.; Hughes, R. P.; Curnow, O. J.; Zheng, X. *Organometallics* **1997**, *16*, 5209.
(50) Drago, R. S. *Physical Methods for Chemists*, 2nd ed.; Saunders College Publishing: Ft. Worth, TX, 1992; pp 135−137.

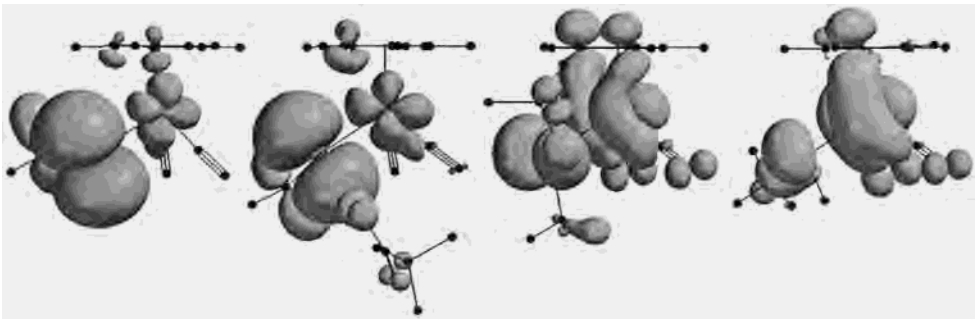

Figure 4. Highest occupied molecular orbitals (HOMOs) of various Brønsted acid adducts of **1(R = Me)** as calculated by the DFT method. Left to right: **1(R = Me)**, **1(R = Me)·TFA**, **1(R = Me)·HBF$_4$**, and **1(R = Me)H$^+$**. Note that the HOMO is largely S in character until the H-bond is polarized toward S, at which time the HOMO becomes largely Fe in character (with concomitant increase in Cp character).

Table 5. Spectroscopic Data for CpFe(CO)$_2$SPh (**1(R = Ph)**) in Various Solvents

solvent	solvent polarity E^N_T	UV−vis (λ_{max}, nm)	IR[a] (ν_{CO}, cm^{-1})
pentane	0.009	582	2035, 1992
benzene	0.111	572	2029, *1985*
tetrahydrofuran	0.207	564	2028, *1988*
dichloromethane	0.309	560	2032, 1985
acetone	0.355	558	2029, 1980
acetonitrile	0.460	552	2031, 1983
1-pentanol	0.568	550	*2032*, 1987
1-butanol	0.602	550	*2033*, 1990
methanol	0.762	542	*2022*, 1985
2,2,2-trifluoroethanol	0.898	<542 sh	2045, *2005*

[a] Italicized vibrational frequencies lie below significant solvent features, and their values are therefore suspect.

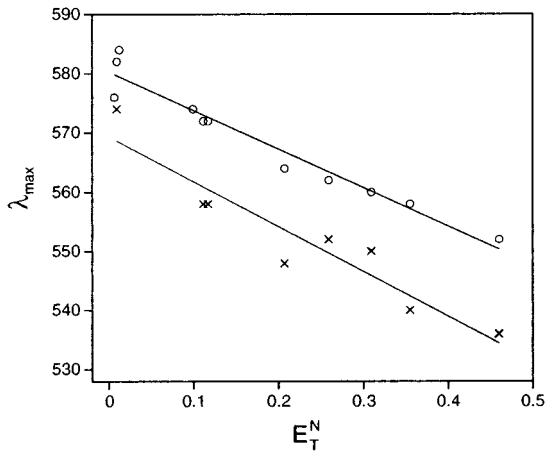

Figure 5. Relationship between the dielectric constant of nonprotic solvents and λ_{max} of the LMCT band of **1(R = Ph)** and **1(R = C$_6$H$_4$-*p*-CF$_3$)** (○ and ×, respectively).

the latter rationalization is suggested by the corresponding values of ν_{co} that indicate specific solute−solvent interactions in the ground state that are not proportional to E^N_T. It is noteworthy that all rubredoxins (Fe$^{II/III}$(cys)$_4$) feature a conserved tyrosine with an arene group that is in close proximity to one of the cysteinate ligands, and deletion of this residue affects the redox potential of the iron center.[51] Thus, specific dipolar solute−solvent dipolar interactions other than hydrogen bonding are capable of modifying the redox properties of metal centers.

Conclusion

We conclude that when the conjugate base of the H-bond donor is a stronger base than the thiolate ligand (as in the present case), H-bond donation has a relatively small effect, but protonation results in a large, discontinuous effect on the electronic structure of **1**. Because protonation depends on the relative basicities of the thiolate ligand and the conjugate base of the H-bond donor, a true continuum of effects can be anticipated only for systems that are p*K*-matched.[52−54] Such a match should permit low-barrier transformation of a π-donor thiolate ligand[55] into a π-acceptor thiol ligand.[56,57] We are currently exploring this hypothesis.

Acknowledgment. The financial support of the National Science Foundation (CHE-9612869), Oklahoma Center for the Advancement of Science and Technology (OCAST HR98-078), and the Petroleum Research Fund (ACS-PRF 35088-AC) is gratefully acknowledged. D.G.M. was the recipient of a Department of Education G.A.A.N.N. Fellowship.

Supporting Information Available: Tables of crystallographic data, fractional coordinates of the non-hydrogen atoms, anisotropic thermal parameters, hydrogen atom parameters, and selected interatomic distances and angles for **1(R = Ph)** and **1(R = Ph)·HBF$_4$**; DFT computed coordinates of **1(R = Me)**, **1(R = Me)H$^+$**, **1(R = Me)·TFA**, and **1(R = Me)·AcOH**; three figures (S1−S3). This material is available free of charge via the Internet at http://pubs.acs.org.

IC011096G

(51) Low, D. W.; Hill, M. G. *J. Am. Chem. Soc.* **1998**, *120*, 11536.
(52) Chen, J. G.; McAllister, M. A.; Lee, J. K.; Houk, K. N. *J. Org. Chem.* **1998**, *63*, 4611.
(53) Kumar, G. A.; McAllister, M. A. *J. Am. Chem. Soc.* **1998**, *120*, 3159.
(54) Cleland, W. W.; Kreevoy, M. M. *Science* **1994**, *264*, 1887.
(55) Ashby, M. T. *Comments Inorg. Chem.* **1990**, *10*, 297.
(56) Kraatz, H. B.; Jacobsen, H.; Ziegler, T.; Boorman, P. M. *Organometallics* **1993**, *12*, 76.
(57) Jacobsen, H.; Kraatz, H. B.; Ziegler, T.; Boorman, P. M. *J. Am. Chem. Soc.* **1992**, *114*, 7851.